Landslide Susceptibility Assessment and Modeling Landslide Volumes Using Geographic Information System (GIS) and Unmanned Aerial Vehicle (UAV): A Case Study in the Xopanac-Apitzato Basin on the Eastern Flank of Iztaccíhuatl Volcano, Puebla, Mexico

Gabriel Legorreta-Paulín, Marcus Bursik, Lilia Arana-Salinas, and Fernando Aceves-Quesada

Abstract

In volcanic mountain terrains, landslides are common and form a major natural hazard, posing risks to human settlements and economic activity. In Mexico, despite the importance of assessing such processes, there are few landslide inventory maps or landslide geo-datasets. Therefore, no practical and standardized methodology has developed to model landslide susceptibility and volume under a Geographic Information System (GIS), and by taking the advantage of Unmanned Aerial Vehicles (UAVs) and their products (aerial photos, orthophotos, dispersed or dense point clouds, and Digital Elevation Models (DEM)). The present text provides an overview of an on-going research project at the Institute of Geography in the National Autonomous University of Mexico (UNAM) presented as an International Programme on Landslides (IPL) project proposal. The aim of this research is to conduct a landslide inventory, produce a landslide susceptibility map, and estimate volume production and distribution within the stream system of the Xopanac-Apitzato watershed. The landslide inventory will be conducted by following the landslide hazard zonation protocol of Washington State DNR. Landslide susceptibility will be conducted by using landforms units and Multiple Logistic Regression. To estimate landslide volume and distribution we will implement the development and adequation of two models by using python.

The watershed is located on the eastern flank of Iztaccíhuatl volcano, the third highest mountain in Mexico. Anthropogenic factors such as land use changes and physiographic factors such as step hillslopes, volcano-tectonic earthquakes, high seasonal precipitation, and disaggregated material predispose the study area to experience episodic evacuation of material through landslide activity. Landslides are common along the stream system, and these slope failures create a potentially hazardous situation for people and property down the valley. In spite of this, there are no landslide inventory maps, and this precludes the mapping of landslide susceptibility and volume. The methodology of the present research encompasses three main levels of analysis. The technique and its implementation in a GIS-based technology is herein presented and discussed. The implementation of the technique yields information essential for policy makers here and in other areas of Mexico.

Keywords

GIS · UAVs · Landslide inventory map · Landslide susceptibility map · Landslide volume · Iztaccíhuatl volcano

G. Legorreta-Paulín (✉)
Instituto de Geografía, Universidad Nacional Autónoma de México, Circuito Exterior, Ciudad Universitaria, Ciudad de México, Mexico

M. Bursik
Department of Geology, University at Buffalo, SUNY Buffalo, Buffalo, NY, USA
e-mail: mib@buffalo.edu

L. Arana-Salinas
Universidad Autónoma de la Ciudad de México, Colegio de Ciencias y Humanidades, Academia de la Licenciatura Protección Civil y Gestión de Riesgos, Ciudad de México, Mexico

F. Aceves-Quesada
Facultad de Ciencias, Universidad Nacional Autónoma de México, Circuito Exterior, Ciudad Universitaria, Ciudad de México, Mexico

B. Abolmasov et al. (eds.), *Progress in Landslide Research and Technology, Volume 4 Issue 1, 2025*, Progress in Landslide Research and Technology, https://doi.org/10.1007/978-3-031-89836-5_13

1 Introduction

In volcanic environments, during the volcanic repose period, small but hazardous landslides and debris flows occur continually. This type of landslide can deliver volumes of some 10–100 m^3 (Montgomery and Dietrich 1994; Pack et al. 2001) and create a potentially hazardous situation for people and property down the valleys, due to the coalescence of upstream landslides that increases the destructive power of debris flows.

Worldwide, landslide cartography has been carried out by using GIS and remote sensing. This cartography is used as a tool to assess the type, distribution, frequency, size, density, geometry, and chronological sequences of landslides. All these attributes are recorded by using historical or multitemporal landslide inventory maps (Washington State Department of Natural Resources (DNR), Forest Practices Division 2006; Hervás and Bobrowsky 2009; Blahut et al. 2010; Guzzetti et al. 2012; Jasiewicz and Stepinski 2013; Slaughter et al. 2017; Du et al. 2020; Shao et al. 2022). To estimate landslide susceptibility, several inventory, heuristic, statistical, and deterministic approaches have been proposed for multiple scopes and spatial scales (Slaughter et al. 2017; Du et al. 2020; Shao et al. 2022). Among the statistical approaches, Multiple Logistic Regression (MLR) is popular for landslide susceptibility assessment because: (1) the evaluation of the model under natural conditions has proven that the model is successful at identifying landslide areas if an adequate set of predictor variables sampling strategy, and sample size are selected (Sujatha and Sridhar 2021; Cemiloglu et al. 2023) and (2) the model has no mechanical meaning, but it explores the relationship between landslide occurrence in the past and the terrain and environmental predictor variables to estimate the probability of landslide (Can et al. 2005; Cemiloglu et al. 2023). Techniques for calculating the volume of material displaced by a landslide in a watershed are based on the physical pre and post-landslide shape obtained by using detailed Digital Elevation Models (DEMs). DEMs could be obtained through the use of differential GPS, Light Detecting and Ranging (LiDAR) or unmanned aerial vehicles (UAVs) (UNEP 2013; Chen et al. 2014; Young 2015; Ray et al. 2020). Also, empirical relationships are established by use of a power-law function that links geometric measurements of landslide area to landslide volume (Peark et al. 2005; Kalderon-Asael et al. 2008; Guzzetti et al. 2009; Wenske et al. 2012). In addition, the distribution of landslide volumes has been determined through historical records, through field identification of the distribution of the materials and through semi-empirical equations that can predict the cross sections and planimetric areas of impact based on the field-estimated volumes (Muñoz-Salinas et al. 2009; Iverson et al. 2015; Andaru et al. 2022).

In Mexico, volcanic regions with stratovolcanoes and monogenetic fields are numerous. Among the three thousand volcanoes in Mexico, dormant stratovolcanoes are common (Centro Nacional de Prevención de Desastres 2001) and can trigger large landslides and debris flows through earthquakes, or in response to heavy rainfall. Despite the importance of assessing such processes, there are few landslide inventory maps derived from geo-datasets using GIS. Also, little work has been done on modelling landside susceptibility and landslide volumes (Capra et al. 2003; Capra and Lugo-Hubp 2006; Pérez-Gutiérrez 2007; Secretaría de Protección Civil 2010).

This is the case for Iztaccíhuatl volcano, the third highest mountain in Mexico (5215.128 m a.s.l.), which has great potential to produce landslides because of its large area of weakened deposits affected by steep slopes, high seasonal rainfall, and tectonic activity. The Río Xopanac-Apitzato on the eastern flank of Iztaccíhuatl volcano has been selected as a case study area. Landslides form major natural hazards in the hilly terrain and cause extensive damage to roads, human settlements, and agricultural land. Therefore, it is important to prepare a landslide inventory map, a susceptibility map, and calculate the volume contributed by landslides to the watershed.

In light of the above, the main goal of this project is to provide standardized methods for conducting landslide inventories, assessing landslide susceptibility, and landslide volumes; this will support governmental authorities in hazard mitigation and landscape planning in Mexico. The Xopanac-Apitzato watershed is selected as a case study area. It is prone to landsliding due to the combination of several factors: volcano-tectonic earthquakes, high precipitation, steep and hilly slopes, loose volcanic deposits, and land use changes.

The methodology encompasses three main levels with several steps of analysis to assess landslide distribution, landslide susceptibility, and volumes. Level 1 builds a historic landslide inventory; Level 2 calculates the landslide susceptibility per landform unit and by using multiple logistic regression (MLR) for the watershed; and Level 3 maps the landslide volume distribution and uses a power law function to estimate the potential total material delivered to the main stream drainage channel by all landslides in the catchment.

2 Method

The overall method followed in this study has 3 major levels with 11 steps (Fig. 1).

Step 1. Selection of a study area: The general procedure is exemplified by a case study on the eastern flank of Iztaccíhuatl

volcano, within Puebla State, Mexico. There, the Xopanac-Apitzato watershed has been selected for landslide mapping, modeling landslide susceptibility, and calculating volumes delivered to its stream system. The study area continually experiences hazardous landslides and debris flows. The study area covers 17.7 km^2 with elevations from 2278 to 3012 m a.s.l. The area is characterized by hilly and steep terrain with slopes between <5° (inner valleys of relatively flat plains) and 66° (mountainous terrain). The Xopanac-Apitzato river is a sub-basin of Río Atoyac, which flows into the Pacific Ocean (Fig. 2).

The stream system of the Xopanac-Apitzato watershed erodes through Tertiary and Quaternary volcanic avalanche deposits, pyroclastic flows, lahars, and fall deposits (García Tenorio 2008).

Along the Xopanac-Apitzato stream system, shallow landslides predominate on steep hills capped by ash and pyroclastic deposits. The steep hills typically experience episodic evacuation of debris by shallow-rapid mass movement followed by slow refilling with colluviums. The debris slides and debris flows are triggered by tecto-volcanic earthquakes, rain, and anthropogenic land use changes (Fig. 3). Active debris slides are abundant on the left hillslopes of the river bank where more anthropic activity takes place (Fig. 4).

Step 2. Background information will be collected to provide context and establish a generalized of landslide processes and to aid analysis, interpretation, and mapping of mass wasting potential within the watershed. Information includes topographic paper maps at scale 1:50,000, and paper maps of geology, land use, climate, and hydrology at

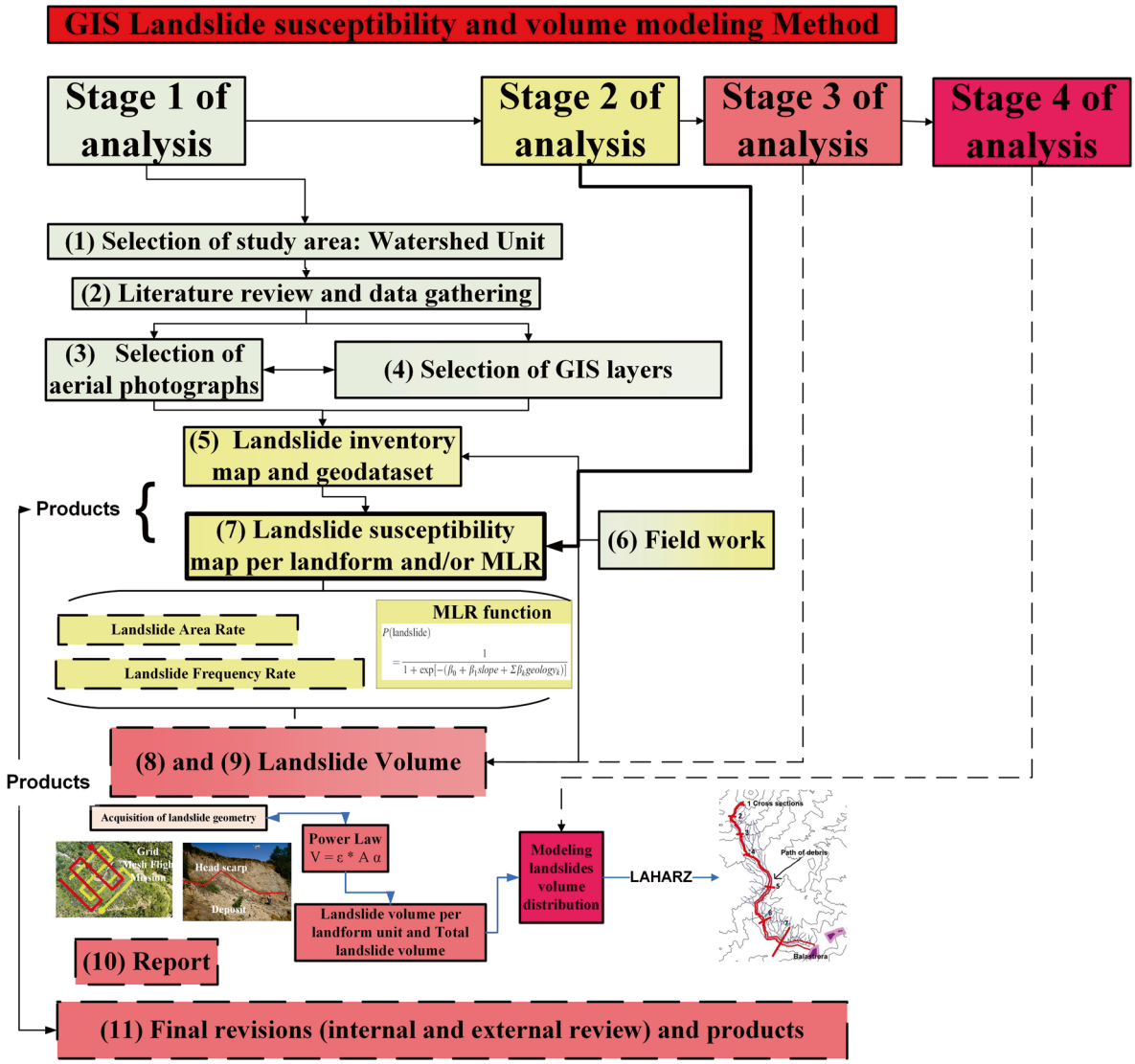

Fig. 1 General procedure for conducting landslide inventories, landslide susceptibility using landforms and MLR statistical method, and landslide volumes calculation

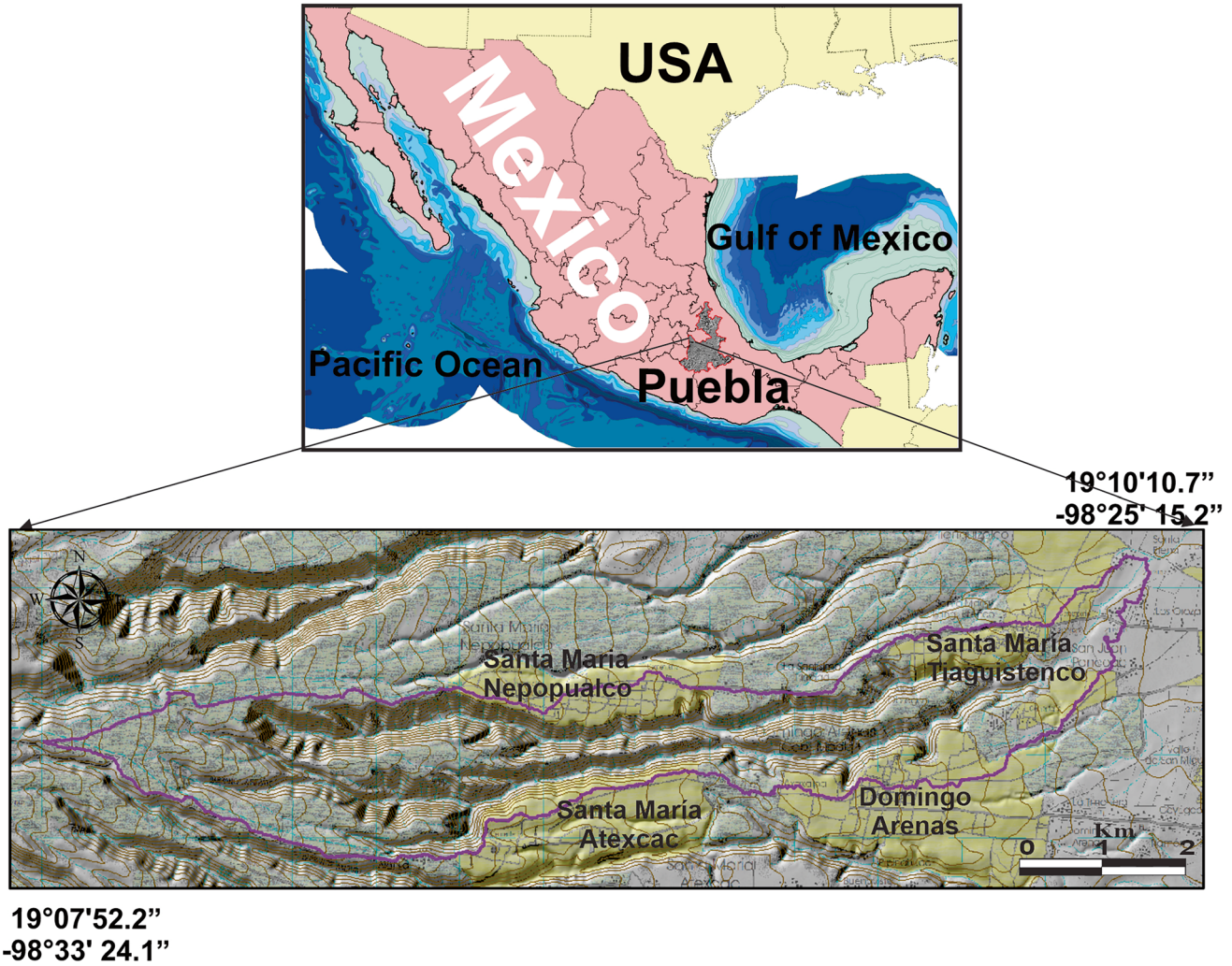

Fig. 2 Study area, Xopanac-Apitzato watershed, State of Puebla, Mexico

scale 1:250,000. All paper maps will be converted to a raster format, georeferenced, and incorporated as GIS layers. Background information also includes orthophotographs at 1:20,000 as well as a 5 m LiDAR digital elevation model (DEM), and its derived thematic maps of slope angle, aspect, curvature, drainage density, and vertical erosion. These topographic derived maps are considered as a good and important controlling predictor factor for landslides. They spatial variations could lead to differences in environmental disturbance and land use patterns that in turn affect the distribution, types, and sizes of landslides. The slope will be mapped in degrees with the ArcGIS slope module. The aspect will be mapped in nine classes to show slope direction terms of degrees from north in a clockwise direction. Terrain curvature is a factor that affects erosion and deposition processes along the hillslope. The curvature map will be calculated with the ArcGIS build-in curvature module and classified into straight and smooth surfaces, concave surfaces, and convex surfaces. The drainage density map will be calculated by splitting the study area into a 1 km^2 grid and obtaining the total length of stream in each. The vertical erosion will be calculated by splitting the study area into a grid of 1 km^2, and the maximum vertical distance between the talweg and the maximum height will be obtained in each cell of the grid.

Step 3. Selection of aerial photographs: In the study area, two sets of aerial photographs will be used: from 1993 and 1995 at a scale of 1:20,000, a Google Earth image from 2001 and an image of 2002 from Planet. The photographs will be analyzed using a mirror stereoscope with 3× magnification and they will be used as a layer during GIS analysis and mapping.

Step 4. Creation of base map using GIS layers: By retrieval and on-off switching of the layers in the GIS system, a base map will be created to assist in the digitizing of landslides and landform units. The digital layers include the watershed boundary, topography, shaded relief, hydrology, roads, geology, and orthophotograph.

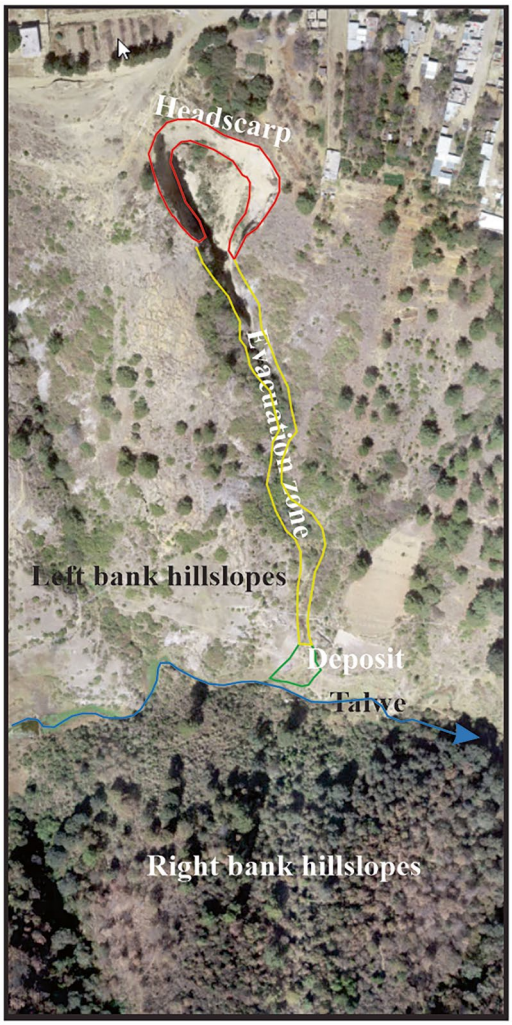

Fig. 3 Debris slide and debris flow in N section of the watershed

Catchment area, stream length, stream patterns, stream orders, drainage density and vertical erosion will be generated from GIS analysis and will be incorporated as background information.

Steps 5 and 6. Landslide map and field work: All landslides will be mapped by "heads-up" digitizing in ArcGIS. This involves mapping on photo-transparencies and digitizing directly onto the screen into GIS at the same scale as the photographs. Landslides will be mapped according to the landslide hazard zonation protocol (2006) of Washington State DNR Forest Practices Division. The protocol classifies landslides into shallow undifferentiated landslides, debris flows, debris slides, deep-seated landslides, earthflows, and rock falls. In the landslide inventory will be mapped for each landslide head scarp, evacuation zone, and deposit (these last two will be not always visible). Some attributes of mapped landslides will be recorded in the GIS database, namely (1) landslide type, (2) landslide size, (3) landslide activity, (4) landslide parts (head scarp, evacuation zone, and deposit), (5) landslide geometry (area, length, width, depth), (6) location of the landslide on the right or left river bank, and (7) certainty of the observation. The interpretation with aerial photographs for landslide mapping will be aided by field work. Two sessions of field work per year will be conducted during the dry and wet season along the main and secondary rivers, for data validation, landslide and landform mapping, verification, and landslide volume measurements.

Step 7. The landslide susceptibility will be modeled by use of landform units and Multiple Logistic Regression (MLR). Once landslides have been mapped, areas of similar landslide potential will be grouped into individual landform units. Landform units will be defined by rules adopted by the Washington Forest Practices Protocol to address landslide

Fig. 4 Debris slide triggered by 2017 earthquake and anthropic activity

hazards (Washington State Department of Natural Resources (DNR), Forest Practices Division 2006).

These landform units are called rule-identified landforms (inner gorges, bedrock hollows, convergent headwalls, outer edges of meanders, and active scarps of deep-seated landslides). Their differentiation is based on slope gradient and shape, lithology, landslide density and sensitivity to forest practices. The aerial photos, the landslide inventory, and GIS layers will be also used to identify other areas that do not meet the rule-identified landform definitions. These areas are called non-rule-identified landforms (such as non-rule-identified inner gorges, non-rule-identified bedrock hollow, steep-gradient hillslopes, moderate-gradient hillslopes, low-gradient hillslopes). Both rule- and non-rule-identified landforms will be entered into GIS as part of a landform polygon feature. For each landform unit, a semi-quantitative hazard rating will be derived from values that correspond to the landslide area rate and the landslide frequency rate; this will lead to an overall hazard rating for each landform and for the watershed.

For MLR analysis, random sampling from landslide areas and non-landslide areas for a training and a validation dataset will be conducted for each thematic independent variable. Assessment of multicollinearity by determination of the variance inflation factor (VIF) and Backward MLR will be conducted on the SPSS statistical package. The variables will be used in MLR to make the final susceptibility map.

To evaluate the models, the "predicted model vs. inventory matching" approach will be used. The percentage of overlay between landform units and MLR model susceptibility maps and the inventory map will be the gauge of how well the models predict the reality. A two-classification scheme (landslide and non-landslide) will be used for the inventory map and model susceptibility maps to facilitate the comparison. The models will be assessed and compared by use of a contingency table and the area under the ROC (receiver operating characteristic) curve (AUC) that shows the amount of overlap and relation between inventory and predicted maps. In the contingency table, the evaluation of the susceptibility model vs. the landslide inventory will be expressed in terms of producer's accuracy (ratio of the number of correctly classified pixels in each category to the total number of true pixels for that category), user's accuracy (ratio of the number of correctly classified pixels in each category to the total number of pixels that are classified by the model in that category), and model efficiency (ratio of correctly minus incorrectly indicated landslide pixels to the total number of true landslide pixels mapped in the inventory map).

In this stage of the project, landform units and MLR susceptibility models will be evaluated to select the one that meets stated criteria for scientific accuracy, technical accessibility, and applicability.

Steps 8 and 9. Landslide volume. Detailed geometric measurements of individual landslides visited during the field work and observed via UAV will indicate the landslide area and volume. The area and volume of the representative landslide head scarp in the watershed will be measured with a UAV. We will exclude the volume and area of the deposits and the slip evacuation area. Geometrical measurement of landslides will be conducted by using a Mavic 3E quadcopter with a camera with 20 megapixels resolution and a CMOS sensor of 1″. Flight planning will used the DJIFlightPlanner software. Aerial images will be acquired with an average flight height of 120 m and at a speed of 7 m/s. The front and side overlaps between aerial photographs will be 80%. We will use a DJI D-RTK 2 base station to obtain a precision of 3 cm during the aerial-photographs capture.

The post-processing of the images will use Agisoft PhotoScan photogrammetric software. We followed a standard post-processing workflow adapted after Ouédraogo et al. (2014). The workflow in PhotoScan will be as follows. (1) Selection and addition of all captured photos for each landslide. (2) Alignment of the loaded aerial photographs. (3) Construction of a cloud of dense point values. (4) Reclassification of the dense point cloud values into ground and the other elements (vegetation, buildings etc.). (5) Creation of a DEM, and 6) creation of an orthophotograph. DEMs at 3 cm per pixel will be obtained.

In ArcMap, the post-sliding topography and the reconstructed pre-sliding topography will be created. This pre-sliding topography will be set heuristically by field observation and reconstruction of the original topography from the post-sliding topography generated by the UAV. The nodes from polygons that represent the current landslide headscarp boundary will be used to create a point file which in turn will be used to extract the elevation data from the DEM for the topography of the landslide. The nodes will be interpolated to create the interpolated pre-sliding topography. The landslide volume will be calculated from the algebraic difference between the reconstructed pre-sliding topography and the actual topography, multiplied by the area of the pixel. To accomplish the above task, we use a model implemented as a tool in ArcGIS called VolumeByInterpolationUNAM-DNRv2.py which calculates the total landslide volume as well as the negative and positive values. Negative values represent accumulation of material in the landslide area while positive values represent loss of material. With the area and volume of the selected landslides an empirical relationship between area and volume will be expressed as a power law with a scaling exponent. This relationship of known landslides will then be used to estimate the potential total material delivered to the main stream drainage channel by all landslides in the watershed. Once the volume has been calculated, a selected landslide will be used to model landslide volume distribu-

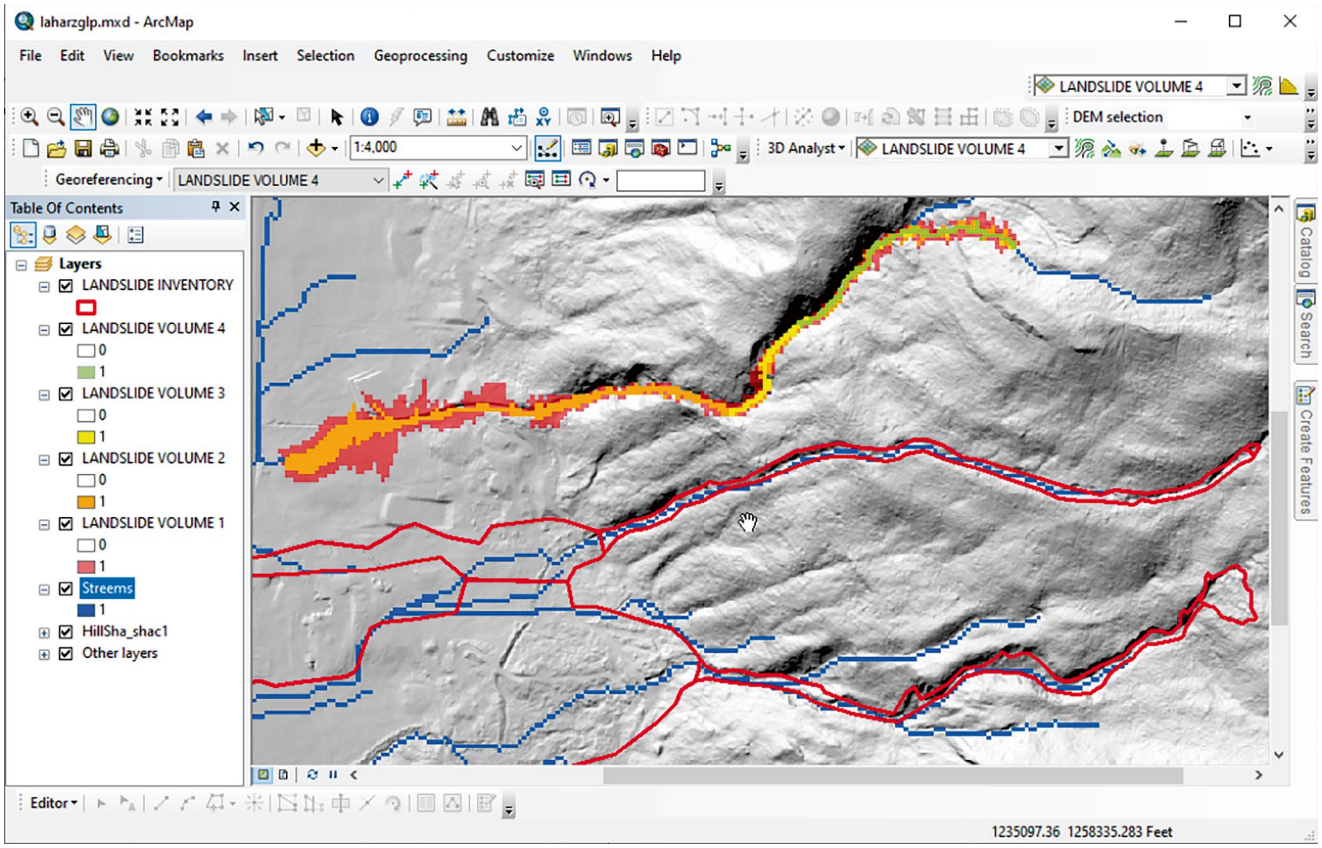

Fig. 5 Theoretical example of 4-volume distribution of a shallow landslide using the adequation of Laharz model

tion. Adequation using Laharz software will allow prediction of areas likely to be at risk (Fig. 5). The adequation is still under development in a program called VolumeDistributionUNAMv0.py.

Step 10. Report: A written report will describe the analysis and include an explanatory text, landform descriptions, landslide triggering mechanisms and the landslide susceptibility and volume findings in the watershed.

Step 11. Final revisions and products: Prior to public release of the report and the corresponding 1:20,000 landslide and landform or MLR susceptibility maps, a tri-level review will be conducted. The first two will be internal peer-reviews carried out by another analyst and a licensed Engineering Geologist. The third review will be external, voluntarily performed by reviewers such as geoscientists, foresters, and other interested parties. The comments received will be used to improve the products prior to final public release on the Institute of Geography website.

Acknowledgments The authors thank authorities from the International Consortium on Landslides (ICL) and the International Programme on Landslides (IPL) for their approval and help.

This research was supported by the Programa de Apoyo a Proyectos de Investigación e Innovación Tecnológica (PAPIIT), UNAM. # IN100223.

Declarations of Interest The authors declare no competing interests.

References

Andaru R, Rau JY, Prayoga AS (2022) Determination of potential secondary lahar hazard areas based on pre- and post-eruption UAV DEMs: automatic identification of initial lahar starting points and supplied lahar volume. Int J Appl Earth Obs Geoinf 115:103096

Blahut J, Van Westen CJ, Sterlacchini S (2010) Analysis of landslide inventories for accurate prediction of debris-flow source areas. Geomorphology 119(1–2):36–51

Can T, Nefeslioglu HA, Gokceoglu C, Sonmez H, Duman TY (2005) Susceptibility assessments of shallow earth flows triggered by heavy rainfall at three catchments by logistic regression analyses. Geomorphology 72:250–271

Capra L, Lugo-Hubp J (2006) Fenómenos de remoción en masa en el poblado de Zapotitlán de Méndez, Puebla: Relación entre litología y tipo de movimiento. Revista mexicana de ciencias geológicas 20(2):95–106

Capra L, Lugo-Hubp J, Borselli L (2003) Mass movements in tropical volcanic terrains: the case of Teziutlán (México). Eng Geol 69:359–379

Cemiloglu A, Zhu L, Mohammednour AB, Azarafza M, Nanehkaran YA (2023) Landslide susceptibility assessment for Maragheh County, Iran, using the logistic regression algorithm. Land 12(7):1397

Centro Nacional de Prevención de Desastres (CENAPRED) (2001) Las cenizas volcánicas del Popocatépetl y sus efectos para la aeronavegación e infraestructura aeroportuaria. Instituto de Geofísica, UNAM, Mexico City

Chen Z, Zhang B, Han Y, Zuo Z, Zhang X (2014) Modeling accumulated volume of landslides using remote sensing and DTM data. Rem Sens 6(2):1514–1537

Du J, Glade T, Woldai T, Chai B, Zeng B (2020) Landslide susceptibility assessment based on an incomplete landslide inventory in the Jilong Valley, Tibet, Chinese Himalayas. Eng Geol 270:105572

García Tenorio F (2008) Avalancha de escombros del pleistoceno tardío del cono Los Pies, complejo volcánico Iztaccíhuatl (Master thesis). Escuela Superior de Ingeniería, Sección de Estudios de Posgrado e Investigación, Unidad Ticomán, Instituto Politécnico Nacional, México, 147 pp

Guzzetti F, Ardizzone F, Cardinali M, Rossi M (2009) Landslide volumes and landslide mobilization rates in Umbria, central Italy. Earth Planet Sci Lett 279:22–229

Guzzetti F, Mondini AC, Cardinali M, Fiorucci F, Santangelo M, Chang KT (2012) Landslide inventory maps: newtools for an old problem. Earth Sci Rev 112:42–66

Hervás J, Bobrowsky P (2009) Mapping: inventories, susceptibility, hazard and risk. In: Sassa K, Canuti P (eds) Landslides—disaster risk reduction. Springer, Berlin, pp 321–349. ISBN 978-3-540-69966-8

Iverson RM, George DL, Allstadt K, Reid ME, Collins BD, Vallance JW, Bower JB (2015) Landslide mobility and hazards: implications of the 2014 Oso disaster. Earth Planet Sci Lett 412:197–208

Jasiewicz J, Stepinski T (2013) Geomorphons—a pattern recognition approach to classification and mapping landforms. Geomorphology 182:147–156

Kalderon-Asael B, Katz O, Aharonov E, Marco S (2008) Modeling the relationship between area and volume of landslides. Geological Survey of Israel. Report (GSI/06/2008), pp 1–16

Montgomery DR, Dietrich WE (1994) A physical based model for the topographic control on shallow landslides. Water Resour Res 30:1153–1171

Muñoz-Salinas E, Castillo-Rodríguez M, Manea V, Manea M, Palacios D (2009) Lahar flow simulations using LAHARZ program: application for the Popocatépetl volcano, Mexico. J Volcanol Geotherm Res 182(1–2):13–22

Ouédraogo MM, Degré A, Debouche C, Lisein J (2014) The evaluation of unmanned aerial system-based photogrammetry and terrestrial laser scanning to generate DEMs of agricultural watersheds. Geomorphology 214:339–355

Pack RT, Tarboton DG, Goodwin CN (2001) Assessing terrain stability in a GIS using SINMAP. In: Proceedings of the 15th annual GIS conference, Vancouver, British Columbia

Peark MR, Ng KY, Zhang DD (2005) Landslide and sediment delivery to a drainage system: some observations from Hong Kong. J Asian Earth Sci 25:821–836

Pérez-Gutiérrez R (2007) Análisis de la vulnerabilidad por los deslizamientos en masa, caso: Tlacuitlapa, Guerrero. Bol Soc Geol Mex 59(2):171–181

Ray RL, Lazzari M, Olutimehin T (2020) Remote sensing approaches and related techniques to map and study landslides. In: Landslides—investigation and monitoring, vol 2. IntechOpen, London, pp 1–25

Secretaría de Protección Civil (2010) Atlas de peligros geológicos e hidrometeorológicos del estado de Veracruz. Comp.: Ignacio Mora González; Wendy Morales Barrera, Sergio Rodríguez Elizarrarás. Xalapa: Secretaría de Protección Civil del estado de Veracruz: Universidad Veracruzana: UNAM. 1V

Shao X, Xu C, Wang P, Li L, He X, Chen Z, Huang Y, Xu X (2022) Two public inventories of landslides induced by the 10 June 2022 Maerkang Earthquake swarm, China and ancient landslides in the affected area. Nat Hazards Res 2(4):269–272

Slaughter SL, Burns WJ, Mickelson KA, Jacobacci KE, Biel A, Contreras TA (2017) Protocol for landslide inventory mapping from lidar data in Washington State: Washington Geological Survey Bulletin 82, 27 p. text, with 2 accompanying ESRI_le geodatabases and 1 Microsoft Excel_le.http://www.dnr.wa.gov/Publications/ger_b82_landslide_inventory_mapping_protocol.zip

Sujatha ER, Sridhar V (2021) Landslide susceptibility analysis: a logistic regression model case study in Coonoor, India. Hydrology 8(1):41

UNEP (2013) A new eye in the sky: eco-drones. UNEP Global Environmental Alert Service. 13 p. http://na.unep.net/geas/getUNEPPageWithArticleIDScript.php?article_id=100. Accesado 10 Feb 2021

Washington State Department of Natural Resources (DNR), Forest Practices Division (2006) Landslide Hazard Zonation (LHZ) mapping protocol, version 2.0. http://www.dnr.wa.gov/BusinessPermits/Topics/LandslideHazardZonation/Pages/fp_lhz_review.aspx

Wenske D, Jen CH, Böse M, Lin JC (2012) Assessment of sediment delivery from successive erosion on stream-coupled hillslopes via a time series of topographic surveys in the central high mountain range of Taiwan. Quat Int 263:14–25

Young AP (2015) Recent deep-seated coastal landsliding at San Onofre State Beach, California. Geomorphology 228:200–212